DOI: https://doi.org/10.24113/ijoscience.v5i7.170

Performance Analysis of Centrifugal Pump at Different Operating Mode

Bhanwar Lal
M.Tech. Scholar
Department of Civil Engineering
Maulana Azad National Institute of Technology
Bhopal, M.P, India
swamibhanwar01@gmail.com

Dr. T. S. Deshmukh
Professor
Department of Civil Engineering
Maulana Azad National Institute of Technology
Bhopal, M.P, India

Abstract: **The aim of this research is to perform numerical simulation of centrifugal pump and PATs mode to analyse its cavitation characteristics and NPSHr at different operating conditions. It was found that maximum efficiency at design discharge for the PAT is about 2% less than the efficiency in pump mode. It is observed that the efficiencies increase steadily on increasing the discharge from 8.88 kg/s to 14.8 kg/s. in both pump and turbine mode. Thereafter the rate of increase in efficiency becomes very less when increase in discharge to 17.76 kg/s. Maximum efficiency of 59.49% being achieved at 14.8 kg/s.**

Keywords: pump, impellor, flow rate, PAT efficiency

I. INTRODUCTION

Pump is a mechanical device that converts mechanical energy taken from an external source into hydraulic energy raising energy level of liquid. Pump can be operated by various prime movers like steam or I.C. engines, compressed air, electric motor, wind or tidal power. Almost all pumps increase the pressure energy of liquid which is subsequently converted into potential energy as the liquid is lifted from a lower to a higher level. The main function of the water pump is to raise the static level of the liquid but some pumps frequently do not lift water at all but they only increase liquid energy. For example- Boiler feed pumps, forced lubrication pumps, firefighting pumps, Booster pumps etc.

Pump As Turbine

Pump as Turbine (PAT) as indicated by name PATs are centrifugal pump used in reverse mode to work as turbine. This technology is very good alternate approach for the generation of electricity replacing conventional turbine. As we are aware that water energy is excessively available apart from small dams in places like canals, water distribution networks, drainage system, natural waterfall etc. The main reason of using pumps to be run as turbine is their availability.

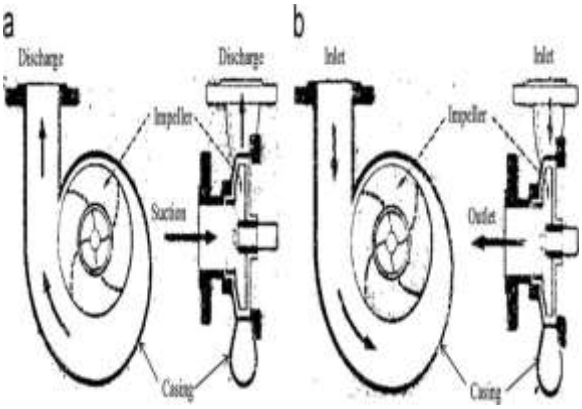

Figure 1: Pump Running in a) Pump Mode b) Turbine Mode

Advantages

1. Construction-Standard pumps are simple and sturdy and do not require highly qualified mechanics for maintenance this makes standard pumps used as turbines more appropriate for developing countries than sophisticated turbines**.**
2. Maintenance-spare parts are readily available in major pump manufacturer's offer after-sales services almost throughout the world and no special equipment and skills required for servicing.

Disadvantages

1. No hydraulic control device: therefore, a control valve must be incorporated in the penstock line (additional costs) to start and stop the PAT. If the valve is used to accommodate to seasonal variations of flow, the hydraulic losses of the installation will increase sharply
2. Peak efficiency: efficiencies of PATs are inferior to sophisticated turbines of the medium to high output range which reach over 90 %. PATs reach efficiencies comparable if notsuperior to locally manufactured Cross Flow or Pelton turbines.

II. LITERATURE REVIEW

[1] The current work deals study Shaft of centrifugal pump for static and dynamic analysis. As we know rotodynamic machineries are designed keenly as there is lot of fluctuation in the loads and speeds. The shaft is analyzed by using finite element analysis technique for stresses and deflections. The total work is carried out in two stages first stage is static analysis. In this stage pump sht is analyzed for stresses and deflection and same results are verified using graphical integration method. And second for dynamic analysis, in this stage result obtained by static analysis are used to calculate dynamic forces coming in pump shaft. Again shaft is analyzed in dynamic input condition and results are verified by using graphical integration method

[2] This paper deals with the design and performance analysis of centrifugal pump. In this paper, centrifugal pump is analyzed by using a single-stage end suction centrifugal pump. A design of centrifugal pump is carried out and analyzed to get the best performance point. The design and performance analysis of centrifugal pump are chosen because it is the most useful mechanical rotodynamic machine in fluid works which widely used in domestic, irrigation, industry, large plants and river water pumping system

[3] The critical review of CFD analysis of centrifugal pumps along with the future scopes for further improvement is presented in this paper. CFD technique has been applied by the researchers to carry out different investigations on centrifugal pumps viz. performance prediction at design and off-design conditions, parametric study, cavitation analysis, diffuser pump analysis, performance of pump running in turbine mode etc.

III.OBJECTIVE OF THE WORK

To perform numerical simulation of centrifugal pump and PATs mode to analyze its cavitation characteristics and NPSHr at different operating conditions

IV.COMPUTATIONAL FLUID DYNAMICS

CFD is a computational technology that is able to study the dynamics of the material that is flowing. The CFD predicts what will happen when the fluids are flooded with or even around the flow of heat, mass transfer, phase change, chemical reaction, mechanical motion, tension and displacement of solids. The basic governing equations are used to analyze any fluid flow problem of Navier-Stoke equations for mass and motion protection

V. METHODOLOGY SOLID MODELING

3D modeling is performed in Ansys ICEM CFD and Ansys BladeGen. The modeled impeller assembly includes the wheel inlet, the hub, the shroud, the blades and the impeller outlet. The modeled assembly of the spiral envelope consists of a housing inlet, a hub, a fairing, a housing wall and a housing outlet. The dimensions of the wheel, casing and intake pipe are as follows:

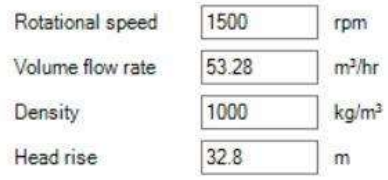

Fig 2: Input Data for Designing

Table I: Dimensions from Vista CPD Empirical Formula

Parameters	Vista CPD	Empirical Formulas
D_1	98.0mm	101.2mm
Cm_1	5.18m/s	4.98m/s
U_1	7.72m/s	8.06m/s
B_1	-	16.36m
D_2	318mm	306.3537mm
Cm_2	-	18.51
U_2	24.85m/s	23.27m/s
B_2	10.1m	9.8m

Dimension of impeller

Dh (mm)	De (mm)	Thk (mm)
28.8	98.0	9.5

D1 (mm)	Cu1 (m/s)	Cm1 (m/s)	U1 (m/s)	W1 (m/s)	β' 1 (deg)	β 1 (de
72.8	0.00	4.24	5.72	7.12	42.15	36.52
85.6	0.00	4.71	6.72	8.20	37.62	35.01
98.3	0.00	5.18	7.72	9.30	33.86	33.86

Fig 3: Impeller Inlet Dimensions

D2 (mm)	B2 (mm)	lean (deg)	β 2 (deg)	W2 (m/s)
316.4	10.1	0.0	11.07	9.57

α 2 (deg)	C2 (m/s)	Wslip/U2	U2 (m/s)	Cu2 (m/s)
6.78	15.57	0.20	24.85	15.46

Fig 4: Impeller Outlet Dimensions

Dimensions of Casing

Dimensions of designed casing are shown below:

Inlet width	20.3	mm	Cutwater clearance	17.2	mm
Base circle radius	175.4	mm	Cutwater thickness	6.6	mm

Sections, cutwater to throat

No.	Area mm²	Centroid radius mm	Outer radius mm	Major radius mm	Minor radius mm	
1	0	175.4	175.4	10.1	0.0	Cutwater
2	143	179.2	184.4	10.1	9.0	
3	289	182.3	191.0	11.1	11.1	
4	440	184.8	195.9	12.8	12.8	
5	594	186.9	200.1	14.4	14.4	
6	750	188.7	203.7	16.0	16.0	
7	909	190.4	207.0	17.4	17.4	
8	1069	191.9	210.1	18.8	18.8	
9	1241	194.9	214.5	20.2	20.2	Throat

Diffuser

Exit Area	1949	mm²	Length	175.4	mm
Exit Hyd Diameter	49.8	mm	Cone angle	3.3	deg

Fig. 5 Dimensions of volute casing from vista CPD

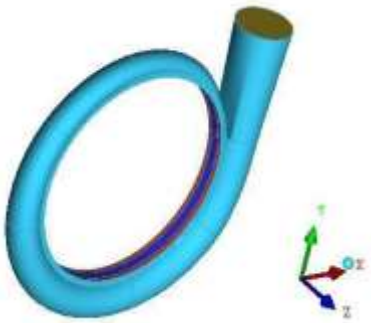

Fig 6: Spiral Casing with Rotation angle 14^0

Dimensions of Inlet Pipe

Diameter of the pipe = 98.0 mm
Length of the pipe = 200 mm

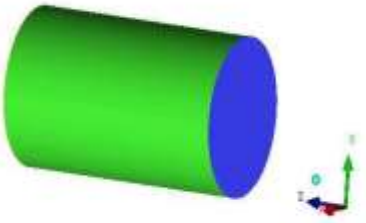

Fig 7: Inlet Pipe

MESH GENERATION

Meshing of Impeller domain

The input of the impeller is connected to the outlet of the pipe and the output of the impeller is connected to the input of the spiral casing through the appropriate interfaces between them. The impeller contains 249618 number of nodes and 1380152 number of tetrahedral elements

Fig. 8: Meshing of Impeller

Meshing of Casing Domain

The domain of the housing comprises a waterproof wall of different areas in cross section, inlet, outlet, hub and cover. The housing input is connected to the

output of the impeller domain through the appropriate interfaces between them. The housing contains 37662 number of nodes and 213813 number of tetrahedral elements

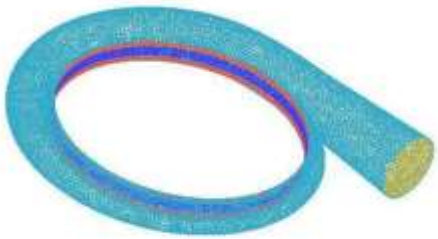

Fig. 9: Meshing of Spiral Casing

Meshing of Inlet Pipe

The input domain comprises an impermeable wall of constant cross-sectional area, inlet and outlet. The output of the pipe is connected to the input of the impeller domain through the appropriate interfaces between them. The pipe contains 26838 number of nodes and 156862 number of tetrahedral elements.

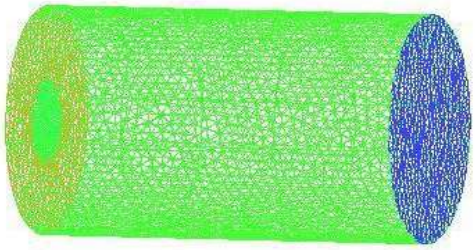

Fig 10: Meshing of Inlet Pipe

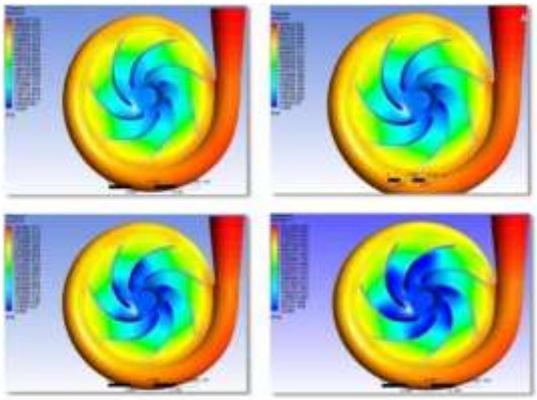

Fig. 11: Pressure Contours for 80% loading and inlet pressure of (a)1atm (b) 0.8atm (c) 0.6atm (d) 0.4atm

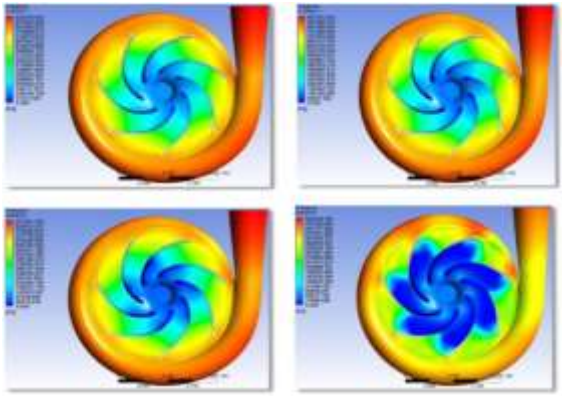

Fig. 12: Pressure Contours for 100% loading and inlet pressure of (a)1atm (b) 0.8 Aatm(c) 0.6atm (d) 0.4at

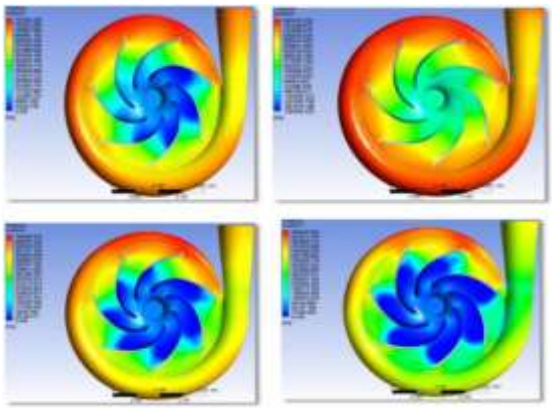

Fig. 13: Pressure Contours for 120% loading and inlet pressure of (a)1atm (b) 0.8atm (c) 0.6atm (d) 0.4atm

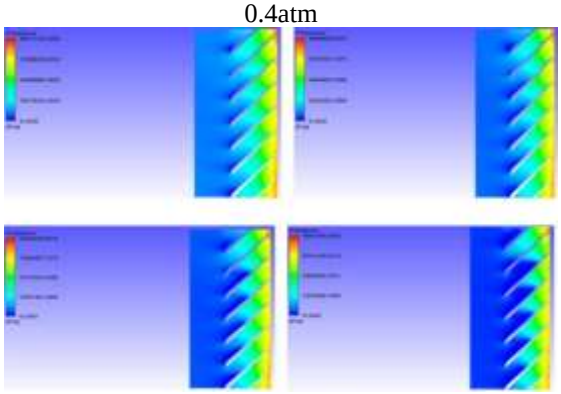

Fig 14: Pressure Contours on blade to blade view for 80% loading and inlet pressure of (a)1atm (b) 0.8atm (c) 0.6atm (d) 0.4atm

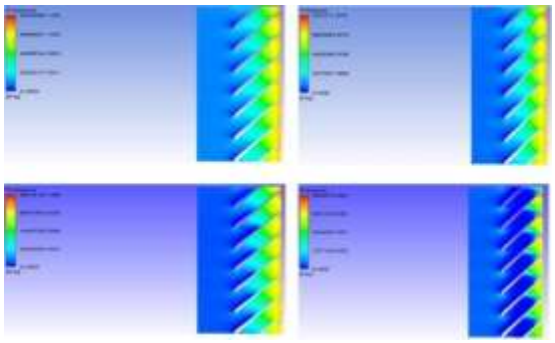

Fig 15: Pressure Contours on blade to blade view for 100% loading and inlet pressure of (a)1atm (b) 0.8atm (c) 0.6atm (d) 0.4atm

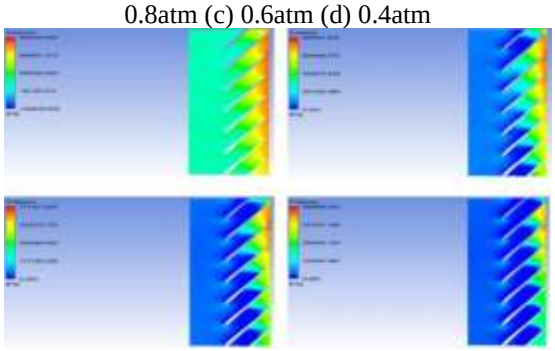

Fig 16: Pressure Contours on blade to blade view for 120% loading and inlet pressure of (a)1atm (b) 0.8atm (c) 0.6atm (d) 0.4atm

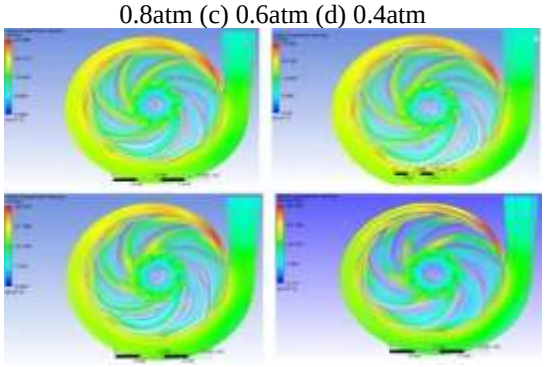

Fig 17: Velocity Streamlines for 80% loading and inlet pressure of (a)1atm (b) 0.8atm (c) 0.6atm (d) 0.4atm

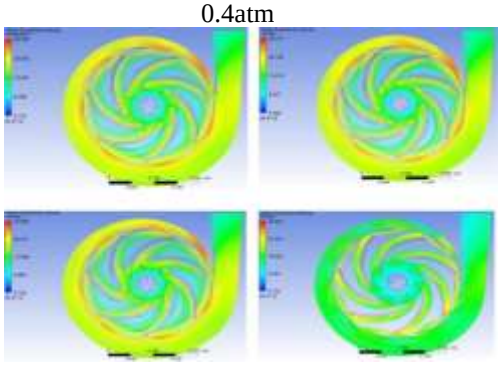

Fig 18 Velocity Streamlines for 100% loading and inlet pressure of (a)1atm (b) 0.8atm (c) 0.6atm (d) 0.4atm

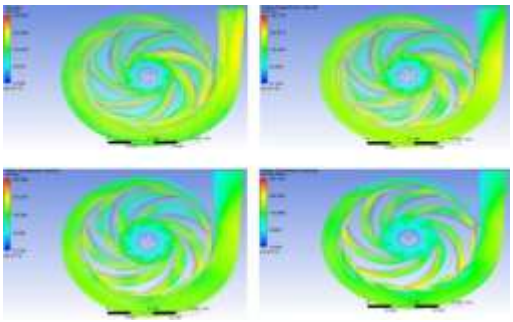

Fig 19: Velocity Streamlines for 120% loading and inlet pressure of (a)1atm (b) 0.8atm (c) 0.6atm (d) 0.4atm

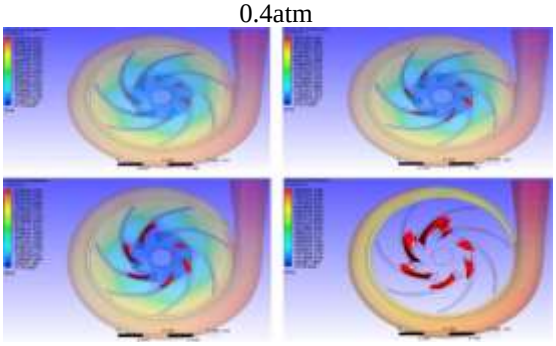

Fig 20: Vapor volume fraction for 80% loading and inlet pressure of (a)1atm (b) 0.8atm (c) 0.6atm (d) 0.4atm

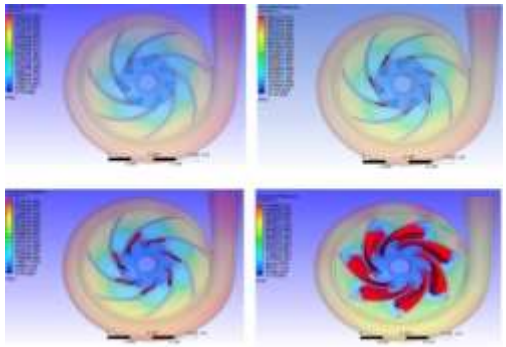

Fig 21: Vapour volume fraction for 100% loading and inlet pressure of (a)1atm (b) 0.8atm (c) 0.6atm (d) 0.4atm

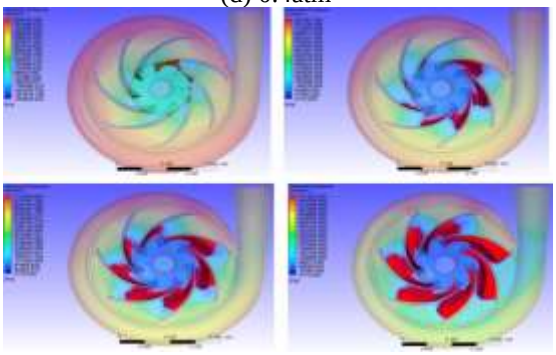

Fig 22: Vapour volume fraction for 120% loading and inlet pressure of (a)1atm (b) 0.8atm (c) 0.6atm (d) 0.4atm

Table II: 60% LOADING (8.88 kg/s)									
Pr given	Pro(Pa)	Pr_i (Pa)	H(m)	T(N/m)	Po(kW)	Pi(kW)	η%	NPSH	σ
0.4	396556	40551.6	37.3718	152.712	23.98	63.3652	37.85	4.033	0.1039
0.6	416821	60816.7	37.8675	150.845	24.014	61.635	38.96	6.099	0.1610
0.8	437086	81081.6	38.0152	148.446	24.098	55.852	43.14	8.1652	0.2147
1	457351	101347	37.9125	148.955	24.048	58.082	41.40	10.23	0.2698

Table III: 80% LOADING (11.74 kg/s)									
Pr given	Pro(Pa)	Pr_i (Pa)	H(m)	T(N/m)	Po(kW)	Pi(kW)	η%	NPSH	σ
0.4	378387	40535.4	36.5473	184.672	29.0036	59.292	48.916	4.288	0.1173
0.6	398652	60800.4	36.57	183.36	29.099	57.839	50.31	6.375	0.1743
0.8	414918	81065	36.6132	182.576	30.009	58.508	51.29	8.186	0.223
1.0	439182	101330	36.6553	182.046	30.182	58.973	51.179	10.27	0.2801

Table IV: 100%LOADING (14.8 kg/s)									
Pr given	Pro(Pa)	Pr_i (Pa)	H(m)	T(N/m)	Po(kW)	Pi(kW)	η%	NPSH	σ
0.4	337620	40478.8	30.1833	192.514	22.131	44.854	49.34	4.379	0.1450
0.6	357886	60743.8	33.1834	210.53	33.072	56.357	58.682	6.744	0.2032
0.8	378090	81013	33.2014	209.981	34.934	56.9638	59.22	8.846	0.2664
1.0	396622	98880.9	33.2122	209.565	33.861	56.917	59.4918	10.575	0.3184

Table V: 120% LOADING (17.76 kg/s)									
Pr given	Pro(Pa)	Pr_i (Pa)	H(m)	T(N/m)	Po(kW)	Pi(kW)	η%	NPSH	σ
0.4	286178	40487.9	18.36	202.554	24.981	48.3696	51.646	4.807	0.2618
0.6	306443	60752.9	24.82	220.679	27.572	51.9070	53.118	6.966	0.2806
0.8	326708	81017.9	27.426	231.82	32.413	57.1003	56.765	8.948	0.3262
1.0	346973	101283	28.9299	221.412	36.412	61.1042	59.59	11.005	0.3804

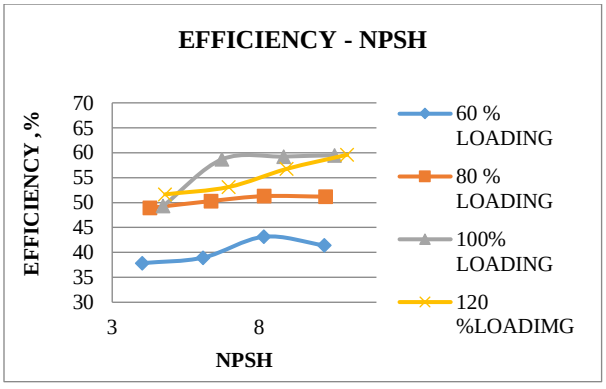

Fig 23: Variation of Efficiency with NPSH at Different loading conditions

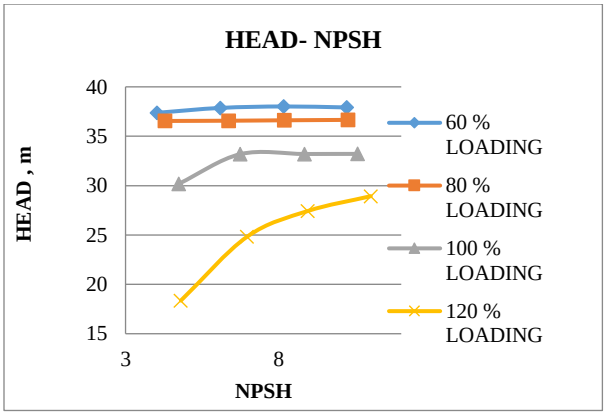

Fig 24: Variation of head with NPSH at Different loading conditions

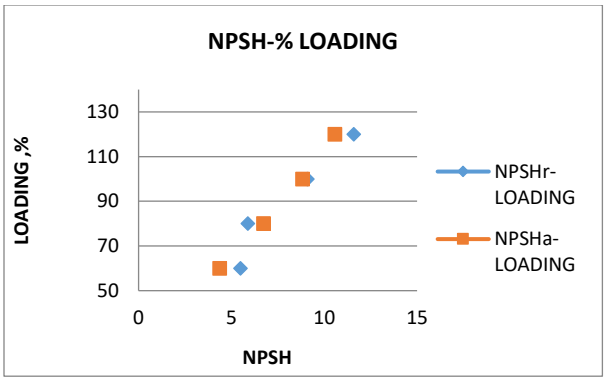

Fig 25: Variation of NPSHr and NPSHA with loading

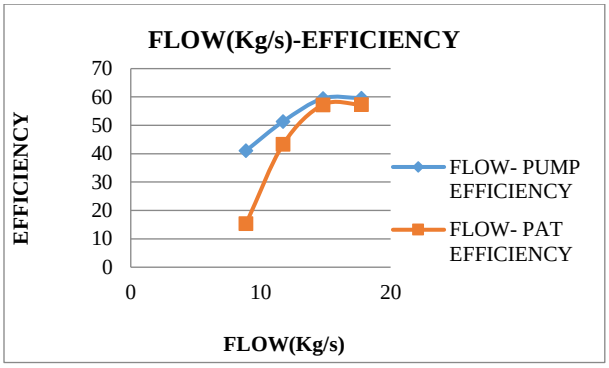

Fig 26: Variation of pump and pat efficiency with flow

VI. CONCLUSIONS

Based on the result of the numerical simulation of flow through pump and PAT. Following conclusions have been drawn.

- Maximum efficiency at design discharge for the PAT is about 2% less than the efficiency in pump mode.
- In case of cavitation the efficiency reduce by about 2% in both pump mode (61.39% -59.49 %) as well as turbine mode (59.42%- 57.31%).
- It is observed that for 60% and 80% loading the head does not varies much with pressure. While for 100% loading the head increase by 10 % for an increase in pressure 0.4 atm to 1 atm. At 120 % loading the increase in head for same for the same pressure variation is about 30%.
- At 1 atm pressure the NPSH value varies by ± 3% for a variation in loading from 60% to 120%.
- The difference between required and available NPSH is minimum at 2.8% for 100% loading. This difference increase to 25% at 60 % loading and 9.6 % at 120 % loading.
- It is observed that the efficiencies increase steadily on increasing the discharge from 8.88 kg/s to 14.8 kg/s. in both pump and turbine mode. Thereafter the rate of increase in efficiency becomes very less when increase in discharge to 17.76 kg/s. Maximum efficiency of 59.49 % being achieved at 14.8 kg/s.

REFERENCES

[1] Pramod J. Bachche, R.M.Tayade, ―Finite Element Analysis of Shaft of Centrifugal Pump‖, IOSR Journal, Volume 7, Issue 3, Aug 2013.

[2] Khin Cho Thin, ―Design and Performance Analysis of Centrifugal Pump‖, World Academy of Science, Engineering and Technology 22 2008, PP. 424-432.

[3] S.R.Shah and S.V.Jain, ―CFD for Centrifugal Pumps‖, Chemical, Civil and Mechanical Engineering Tracks of 3rd Nirma University International Conference (NUiCONE 2012), PP. 135-140.

[4] W.K. Chan, ―The flow patterns within the impeller passages of a centrifugal blood pump model‖, Medical Engineering & Physics 22 (2000), PP. 381–393.

[5] Austin H Church, ―Centrifugal pumps and blowers‖, John Willey & son's publication, 1st edition, 1944.

[6] John S. Anagnostopoulos, ―CFD analysis and design effects in a radial pump impeller‖, Wseas transactions on fluid mechanics, Issue 7, Vol.-1, July 2006.

[7] A Shyam Prasad, BVVV Lakshmipathi Rao, A Babji, Dr P Kumar Babu, ―Static and Dynamic Analysis of a Centrifugal Pump Impeller‖, IJSER, Volume 4, Issue 10, October 2013.

[8] Karan Rajdev, ―Pressure and stress distribution analysis of centrifugal pump‖, Thapar University, Patiyala, June 2008.

[9] Mario Savar and Hrvoje Kozmar, ―Improving centrifugal pump efficiency by impeller trimming‖, Desalination 249 (2009), PP. 654– 659.

[10] Ramesh Agarwal and Ling Zhou, ―Numerical and Experimental Study of Axial Force and Hydraulic Performance in a Deep-Well Centrifugal Pump with Different Impeller Rear Shroud Radius‖, Fluids Engineering Division of ASME OCTOBER 2013, Vol. 135, PP. 654-670.

[11] Bruce R. Munson, et al., ―Fundamentals of Fluid Mechanics, ‖ John Wiley & Sons, Inc. 6th edition 2009, PP. 653-662.